Symbol-level Precoding for Multi-cell ISAC

Nithin Babu
Dept. EEE, University College London
n.babu@ucl.ac.uk

Christos Masouros
Dept. EEE, University College London
c.masouros@ucl.ac.uk

Abstract—This paper proposes symbol-level precoder (SLP) designs for a multi-cell multi-input single-output (MISO) integrated sensing and communication (ISAC) system under different levels of coordination among the base stations (BSs). Namely, we consider the BSs operating under coordinated beamforming (CBF) and coordinated multipoint (CoMP) schemes. In the former, channel state information (CSI) is shared, while in the latter, both CSI and user data are shared. The formulated optimization problems to maximize the weighted combination of the Fisher information value (FIV) and the minimum-signal-to-interference-plus-noise-ratio (SINR) are represented in the semidefinite relaxed (SDR) form and solved using an alternate optimization (AO) algorithm. The proposed solutions show improved performance compared to the baseline block-level precoding counterparts.

Index Terms—Integrated Sensing and Communication, Cramer-Rao bound, CoMP, CBF

I. INTRODUCTION

A common property to realize the next-generation wireless network's location-based services, such as connected vehicles and remote healthcare, is the communication network possessing radio sensing capability [1]. A high-resolution sensing requires large bandwidth and multiple antennas, which are expected to be a part of the 5G advanced and 6G networks [2]. Moreover, the high path loss in the proposed higher-frequency bands reduces the coverage area, demanding small-cell deployments that increase the chances of line-of-sight (LoS) links to the users/targets. Hence, the next-generation mobile communication network, hereafter referred to as an Integrated Sensing and Communication (ISAC) system, has the potential to do radio frequency (RF) sensing in addition to serving the users.

The idea of an ISAC system has gained much attention lately from academia [1] and industry [3]. In this work, we consider one of the challenges in realizing a multi-cell ISAC system: designing an optimal transmit symbol vector tailored to both the sensing and communication performance matrices by considering inter-cell communication and sensing links. Unlike the single-cell system, a multi-cell system has interfering sensing and communication links from the neighbouring BSs. The additional signal power received through these links can adversely affect the performance of an ISAC system. This demands varying levels of coordination among the BSs.

In a communication-only multi-cell setup, the base stations (BSs) can either share the observed channel state information (CSI) or the CSI and the user data. The former coordination

scheme is called coordinated beamforming (CBF), whereas the latter is called coordinated multipoint (CoMP) [4]. We extend these coordination schemes to a multi-cell ISAC setup by adding the additional overhead of sharing the inter-cell reflection directions, in which a BS sees the neighbouring BSs' targets.

Various multi-cell ISAC setups have been considered in the literature, as documented in [3], [5]–[11]. The models put forth in [3], [5]–[10] utilize either orthogonal schemes, CoMP, or CBF for ISAC. However, these models do not provide a general framework that accounts for the fact that inter-cell reflections can either enhance or degrade sensing performance, depending on the level of coordination among BS. Our previous work, [11], proposes such a framework for block-level precoding (BLP), and the results there indicate that when appropriately coordinated, as in the CoMP scenario, the sensing performance can be improved by leveraging the additional signal power received through inter-cell links, as opposed to the CBF scheme, while guaranteeing a given communication performance. In this work, we consider a different precoding scheme called symbol level precoding (SLP) that can potentially leverage interference to enhance the signal reception at a communication user. The basic idea is that the transmit symbol vector is designed in a way to ensure that the rotated version of the received symbol at each user falls in the constructive interference (CI) region of the corresponding transmitted symbol [12]. Unlike the BLP scheme, the SLP scheme, for instance, in the CoMP mode, exploits the intracell and inter-cell interferences. Consequently, the SLP solutions are expected to give a better ISAC performance for a given power budget. Moreover, the SLP scheme designs the transmit symbol vector from which the precoders can be derived as explained in [12]. In this work, we design the transmit symbol vector that maximizes a weighted combination of sensing and communication performance metrics. We use the Fisher information value (FIV), whose inverse gives the Cramer-Rao bound, for measuring the sensing performance, whereas the minimum signal-to-interference-plus noise ratio (SINR) is used as the communication performance metric.

II. SYSTEM MODEL

We consider a multi-cell ISAC system with J cells and K users and one target per cell; each BS is equipped with a uniform linear array (ULA) of N_t transmit antennas spaced at $\lambda/2$ distance, where λ is the wavelength. Additionally, the BS has a N_r-element receive ULA with an inter-element
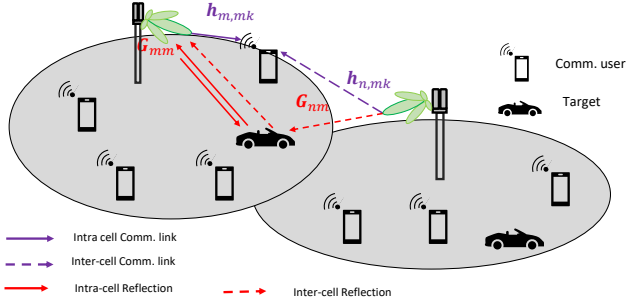
Fig. 1: System setup.

Fig. 2: Illustration of CI condition.

spacing of $\lambda/2$ antennas isolated from the transmit ULA. The mth BS transmits a narrowband signal matrix, $\mathbf{X}_m = [\mathbf{x}_{m1}, \mathbf{x}_{m2}, ..., \mathbf{x}_{mL}] = [\mathbf{w}_{m1}, \mathbf{w}_{m2}, .., \mathbf{w}_{mK}]\mathbf{S}_m \in \mathcal{C}^{N_{\text{t}} \times L}$, to the users in the cell, with $L > N_{\text{t}}$ being the length of the radar pulse/ communication frame. Here, $\mathbf{w}_{ml} \in \mathcal{C}^{N_{\text{t}} \times 1}$ represents the precoder vector for the lth user of the mth BS and $\mathbf{S}_m \in \mathcal{C}^{K \times L}$ is the orthogonal data stream transmitted to K users of the mth BS. As shown in Fig. 1, a BS receives its echo signal and multiple echo signals from its target due to inter-cell reflection (ICR) from the neighbouring BSs. The resulting echo signal received by the mth BS from the target in its cell is given as

$$\mathbf{Y}_m^{\text{R}} = \mathbf{G}_{mm}\mathbf{X}_m + \sum_{n \neq m}^{J} \mathbf{G}_{nm}\mathbf{X}_n + \mathbf{Z}_m^{\text{R}}, \quad \forall m, \qquad (1)$$

where $\mathbf{G}_{nm} = \alpha_{nm}\mathbf{a}_{mm}\mathbf{v}_{nm}^{\text{T}}\ \forall n = \{1, 2, .., J\} \equiv \mathcal{J}$, is the target response matrix at the mth BS due to the transmission from the nth BS in which $\mathbf{a}_{m,m}$ and $\mathbf{v}_{nm}$ are the array response vectors in the directions θ_{mm} and θ_{nm}, respectively, and $()^{\text{T}}$ represents the transpose operation. Here, $\alpha_{n,m}$ represents the complex amplitude of the received signal and $\mathbf{Z}_m^{\text{R}} \in \mathcal{C}^{N_{\text{r}} \times L}$ is an additive white Gaussian noise (AWGN) matrix with the variance of each entry being σ_{R}^2. Equation (1) assumes that all the neighbouring BSs have a LoS link to the mth BS's target. The first term on the right-hand side (RHS) of (1) is called intra-cell reflection due to the signal vector from the same BS, whereas the second term represents inter-cell reflection (ICR) due to the signals from the neighbouring BSs.

Let U_{mk} represents the kth user of the mth BS. If the sth transmitted symbol by the mth BS to U_{mk} is M-PSK-modulated: $d_{mks} = de^{j\phi_{mks}}$, the received symbol at U_{mk} is

$$y_{mks}^{\text{C}} = \mathbf{h}_{m,mks}^{T}\mathbf{x}_{ms}d_{mks} + \sum_{n \neq m}^{J} \mathbf{h}_{n,mks}^{T}\mathbf{x}_{ns}d_{nks} + z_{mk}^{\text{C}}, \quad (2)$$

where $\mathbf{h}_{n,mks}^{T} = \mathbf{h}_{n,mk}^{T}e^{j(-\phi_{nks})}$, $\mathbf{x}_{ns} = \sum_{l=1}^{K}\mathbf{w}_{nl}e^{j(\phi_{nls})}$, and z_{mk}^{C} represents AWGN noise with a variance of σ_{C}^2. In (2), the first term is a scaled and rotated version of the desired symbol d_{mks}, and the second term is the inter-cell interference from the neighbouring BSs.
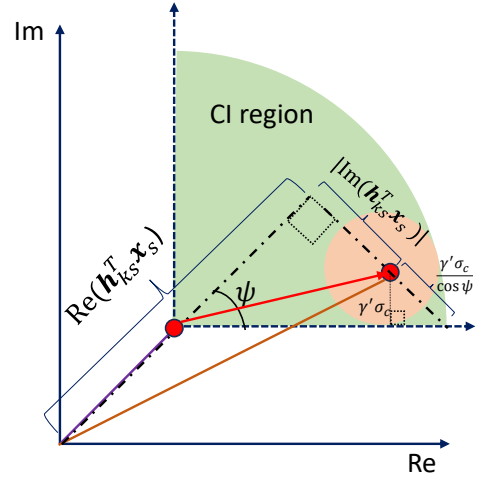
A. Preliminaries on Symbol Level Precoding

This paper utilizes SLP to design the transmit symbol vector, simultaneously enhancing both sensing and communication performance metrics. SLP harnesses co-channel interference in a constructive manner to enhance the received signal power. It does so by instantly aligning the interference signals with the desired signal at the receiver end. As shown in Fig. 2, each transmitted symbol possesses a CI region. SLP designs the transmit symbol vector to ensure that the symbol received at the receiver, comprising both the desired and interfering symbols, falls within the CI region of the desired symbol. For a single-cell system ($J = 1$), this criterion is met by satisfying the geometric condition given in (3), derived from Fig. 2 [13]. We refer the readers to [14] for a detailed discussion on SLP.

$$\left(\left|\text{Im}\left\{\mathbf{h}_{m,mks}^{T}\mathbf{x}_s\right\}\right| - \left(\text{Re}\left\{\mathbf{h}_{m,mks}^{T}\mathbf{x}_s\right\}\right)\tan\psi + \gamma'\sigma_{\text{C}}\frac{1}{\cos\psi}\right) \leq 0. \tag{3}$$

Here, $\psi = \pi/M_{\text{psk}}$ where M_{psk} represents the modulation order of the PSK scheme employed and $\gamma' = \sqrt{\gamma}$ where γ denotes the minimum communication SINR.

III. TRANSMIT SYMBOL VECTOR DESIGN BASED ON SYMBOL-LEVEL PRECODING

This section explains how the transmit symbol vector is designed using SLP when the BSs coordinate under the CBF and CoMP schemes.

A. Coordinated Beamforming

Recall that in the CBF scheme, the BSs do not share data among themselves. Hence, the SLP design can only align the intra-cell interference to enhance the received signal power, whereas the inter-cell interference degrades the SINR value. The corresponding SINR constraint is derived from (3) as (4).

$$\left(\left| \text{Im}\left\{ \mathbf{h}_{m,mks}^T \mathbf{x}_{ms} \right\} \right| - \left(\text{Re}\left\{ \mathbf{h}_{m,mks}^T \mathbf{x}_{ms} \right\} \right) \tan\psi + \gamma' \left(\sqrt{\left(\sigma_C^2 + \sum_{n \neq m}^{J} |\mathbf{h}_{n,mk}^T \mathbf{x}_{ns}|^2 \right)} \right) \frac{1}{\cos\psi} \right) \leq 0 \; \forall k, s \tag{4}$$

We assume each BS estimates its target's angle θ_{mm} from the received signal (1). The FIV, whose inverse gives the CRB in estimating θ_{mm}, is given in [11] as

$$F_{m,\text{cbf}} = 2\,\text{Re}\left\{ \text{tr}\left(\frac{d\boldsymbol{\mu}_{m,\text{cbf}}^H}{d\theta_{mm}} \mathbf{C}_{m,\text{cbf}}^{-1} \frac{d\boldsymbol{\mu}_{m,\text{cbf}}}{d\theta_{mm}} \right) \right\}. \tag{5}$$

where, $\boldsymbol{\mu}_{m,\text{cbf}} = \mathbf{G}_{mm}\mathbf{X}_m$ and

$$\mathbf{C}_{m,\text{cbf}} = \sum_{n \neq m}^{J} \mathbf{G}_{nm}\mathbf{X}_n\mathbf{X}_n^H\mathbf{G}_{nm}^H + \sigma_R^2\mathbf{I}_{N_r} \tag{6}$$

Using the definitions of $\mathbf{G}_{m,m}$, we have,

$$\frac{1}{L\alpha_{mm}^2}\text{tr}\left(\frac{d\boldsymbol{\mu}_{m,\text{cbf}}^H}{d\theta_{mm}} \mathbf{C}_{m,\text{cbf}}^{-1} \frac{d\boldsymbol{\mu}_{m,\text{cbf}}}{d\theta_{mm}} \right)$$
$$= (\dot{\mathbf{a}}_{mm}^H\mathbf{C}_{m,\text{cbf}}^{-1}\dot{\mathbf{a}}_{mm}) \cdot (\mathbf{v}_{mm}^H\mathbf{R}_{\mathbf{X}_m}^*\mathbf{v}_{mm})$$
$$+ (\dot{\mathbf{a}}_{mm}^H\mathbf{C}_{m,\text{cbf}}^{-1}\mathbf{a}_{mm}) \cdot (\mathbf{v}_{mm}^H\mathbf{R}_{\mathbf{X}_m}^*\dot{\mathbf{v}}_{mm})$$
$$+ (\mathbf{a}_{mm}^H\mathbf{C}_{m,\text{cbf}}^{-1}\dot{\mathbf{a}}_{mm}) \cdot (\dot{\mathbf{v}}_{mm}^H\mathbf{R}_{\mathbf{X}_m}^*\mathbf{v}_{mm})$$
$$+ (\mathbf{a}_{mm}^H\mathbf{C}_{m,\text{cbf}}^{-1}\mathbf{a}_{mm}) \cdot (\dot{\mathbf{v}}_{mm}^H\mathbf{R}_{\mathbf{X}_m}^*\dot{\mathbf{v}}_{mm}) \tag{7}$$

where $\mathbf{R}_{\mathbf{X}_m} = \frac{1}{L}\mathbf{X}_m\mathbf{X}_m^H = \frac{1}{L}\sum_{s=1}^{L}\mathbf{R}_{\mathbf{X}_{ms}}$ and $()^*$ represents the conjugate of the operand. Here, $F_{m,\text{cbf}}$ is obtained by substituting (6) and (7) in (5). Note that (5) is the result of the observation that $\text{vec}(\mathbf{Y}_m^R)$ is a multi-variate Gaussian random variable with mean $\boldsymbol{\mu}_{m,\text{cbf}}$ and covariance matrix $\mathbf{C}_{m,\text{cbf}}$. Consequently, we formulate the optimization problem as

$$\text{(P1): } \underset{\{\mathbf{x}_{ms}\},\{\mathbf{R}_{\mathbf{X}_{ms}}\}}{\text{maximize}} \quad \frac{F_{m,\text{cbf}}\,\rho}{\text{NF}_{R,\text{cbf}}^{\text{slp}}} + \frac{(1-\rho)\gamma'}{\text{NF}_{C,\text{cbf}}^{\text{slp}}},$$

$$\mathbf{v}_{mn}^T\frac{1}{L}\sum_{s}^{L}\mathbf{R}_{\mathbf{X}_{ms}}\mathbf{v}_{mn}^* \leq P_{m,\text{leak}}, \quad \forall n, \tag{8a}$$

$$\begin{bmatrix} \mathbf{R}_{\mathbf{X}_{ms}} & \mathbf{x}_{ms} \\ \mathbf{x}_{ms}^H & 1 \end{bmatrix} \geq 0; \; \mathbf{R}_{\mathbf{X}_{ms}} \geq 0 \; \forall s, \tag{8b}$$

$$\frac{1}{L}\text{tr}\left(\sum_{s=1}^{L}\mathbf{R}_{\mathbf{X}_{ms}} \right) \leq P_t, \tag{8c}$$

$$(4). \tag{8d}$$

where $\rho \in [0,1]$ is the weighting factor and $A \geq 0$ represents the positive-semidefinite constraint on the matrix A. The constants $\text{NF}_{R,\text{cbf}}^{\text{slp}}$ and $\text{NF}_{C,\text{cbf}}^{\text{slp}}$ are the respective normalization factors obtained by setting $\rho = 1$ and $\rho = 0$. The normalization factors will scale down the sensing and communication performance values to fit within the range of $[0,1]$. Equation (8a) restricts the power leaked to a neighbouring Bs's target to be less than or equal to a given value $P_{m,\text{leak}}$ and (8b) represents the relaxed constraint $\mathbf{R}_{\mathbf{X}_{ms}} \geq \mathbf{x}_{ms}\mathbf{x}_{ms}^H$. Equation (8c) ensures the total radiated power remains below P_t. Problem (P1) is

non-convex because of the non-convex form of $\mathbf{C}_{m,\text{cbf}}$ in $F_{m,\text{cbf}}$ and the non-convex SINR constraint (4). We solve (P1) by solving the following two problems alternatively until convergence

$$\text{(P1.1): } \underset{\{\mathbf{x}_{ms}\},\{\mathbf{R}_{\mathbf{X}_{ms}}\}}{\text{maximize}} \quad \frac{\rho F_{m,\text{cbf}}}{\text{NF}_{R,\text{cbf}}^{\text{slp}}} + \frac{(1-\rho)\gamma'}{\text{NF}_{C,\text{cbf}}^{\text{slp}}},$$

$$(8a), (8b), (8c) \tag{9a}$$

$$\left| \text{Im}\left\{ \mathbf{h}_{m,mks}^T\mathbf{x}_{ms} \right\} \right| - \left(\text{Re}\left\{ \mathbf{h}_{m,mks}^T\mathbf{x}_{ms} \right\} \right)\tan\psi$$
$$+ \gamma'\left(\sqrt{\left(\sigma_C^2 + I^2 \right)} \right)\frac{1}{\cos\psi} \leq 0 \; \forall k, s \tag{9b}$$

$$\|\mathbf{h}_{m,nks}^T\mathbf{x}_{ms}\| \leq \frac{I}{\sqrt{J-1}} \tag{9c}$$

$$\text{(P1.2): } \underset{\{\mathbf{x}_{ms}\},\{\mathbf{R}_{\mathbf{X}_{ms}}\}}{\text{minimize}} \quad \frac{P_{\text{leak}}}{4\pi P_t} + \frac{I_m^2}{I_{\max}^2}$$

$$F_{m,\text{cbf}} \geq \hat{F}_{m,\text{cbf}} \; \forall m \tag{10a}$$

$$\mathbf{v}_{mn}^T\frac{1}{L}\sum_{s}^{L}\mathbf{R}_{\mathbf{X}_{ms}}\mathbf{v}_{mn}^* \leq P_{m,\text{leak}} \tag{10b}$$

$$\left| \text{Im}\left\{ \mathbf{h}_{m,mks}^T\mathbf{x}_{ms} \right\} \right| - \left(\text{Re}\left\{ \mathbf{h}_{m,mks}^T\mathbf{x}_{ms} \right\} \right)\tan\psi$$
$$+ \hat{\gamma}'\left(\sqrt{\left(\sigma_C^2 + I^2 \right)} \right)\frac{1}{\cos\psi} \leq 0 \; \forall k, s \tag{10c}$$

$$\|\mathbf{h}_{m,nks}^T\mathbf{x}_{ms}\| \leq \frac{I_m}{\sqrt{J-1}}; \; I_m \leq I \tag{10d}$$

$$(8b) \tag{10e}$$

Problem (P1.1) maximizes the objective for a given sensing and communication leakage bounds $P_{m,\text{leak}}$ and I, whereas (P1.2) minimizes the sensing and communication leakages for a given $\hat{F}_{m,\text{cbf}}$ and $\hat{\gamma}'$ values obtained by solving (P1.1). Here, $I = \max\{I_m\}$ and $I_{\max}$ is the maximum interference value necessary to ensure the normalization of the sensing objective. Note that using (9b) and (9c), we represent the SINR constraint (4) as a leakage constraint which restricts the inter-cell interference received at any user to less than I^2. The value of I^2 is minimized in (P1.2). The initial value of I^2 determines the convergence speed of the algorithm: a high value results in a slow convergence, whereas a low value will result in an underutilization of the available power budget. Both are convex optimization problems that can be solved using the available solvers, such as Matlab's CVX.

B. Coordinated Multipoint

Since the BSs share the user data and the CSI in the CoMP mode, the $J \cdot K$ users in the multi-cell ISAC system can be considered to be served by a virtual single-cell BS with $N = J \cdot N_t$ antennas. Let $\mathbf{h}_k \in \mathcal{C}^{N \times 1}$ be the actual channel vector

from all the BSs to U_k. The received signal at U_k is expressed as

$$\mathbf{y}_k^{\mathrm{C}} = \mathbf{h}_k^T \mathbf{X} + \mathbf{z}_k^{\mathrm{C}}, \ \forall U_k, \tag{11}$$

where $\mathbf{X} = [\mathbf{X}_1; \mathbf{X}_2, ...; \mathbf{X}_J] \in \mathcal{C}^{N \times L}$ is the concatenated symbol matrix available at each BS and $\mathbf{z}_k^{\mathrm{C}} \in \mathcal{C}^{1 \times L}$ is an AWGN noise vector with variance of each entry being σ_{C}^2. Adapting (5) to the CoMP case, for $m, n \in \{1, 2\}$ and $m \neq n$, $J = 2$, we get,

$$\mathrm{tr}\left\{\frac{d\boldsymbol{\mu}_{m,\mathrm{CoMP}}}{d\theta_{mm}}^H \mathbf{C}_{m,\mathrm{cmp}}^{-1} \frac{d\boldsymbol{\mu}_{m,\mathrm{CoMP}}}{d\theta_{mm}}\right\}$$

$$= L\alpha_{m,m}^2 (\dot{\mathbf{a}}_{mm}^H \mathbf{C}_{m,\mathrm{cmp}}^{-1} \dot{\mathbf{a}}_{mm}) \cdot (\mathbf{v}_{mm}^{'H} \mathbf{D}_m \mathbf{R}_\mathbf{X}^* \mathbf{D}_m^H \mathbf{v}_{mm}^{'})$$

$$+ L\alpha_{mm}^2 (\dot{\mathbf{a}}_{mm}^H \mathbf{C}_{m,\mathrm{cmp}}^{-1} \mathbf{a}_{mm}) \cdot (\mathbf{v}_{mm}^{'H} \mathbf{D}_m \mathbf{R}_\mathbf{X}^* \mathbf{D}_m^H \dot{\mathbf{v}}_{mm}^{'})$$

$$+ L\alpha_{mm}^2 (\mathbf{a}_{mm}^H \mathbf{C}_{m,\mathrm{cmp}}^{-1} \dot{\mathbf{a}}_{mm}) \cdot (\dot{\mathbf{v}}_{mm}^{'H} \mathbf{D}_m \mathbf{R}_\mathbf{X}^* \mathbf{D}_m^H \mathbf{v}_{mm}^{'})$$

$$+ L\alpha_{mm}^2 (\mathbf{a}_{mm}^H \mathbf{C}_{m,\mathrm{cmp}}^{-1} \mathbf{a}_{mm}) \cdot (\dot{\mathbf{v}}_{mm}^{'H} \mathbf{D}_m \mathbf{R}_\mathbf{X}^* \mathbf{D}_m^H \dot{\mathbf{v}}_{mm}^{'})$$

$$+ L\alpha_{nm}\alpha_{mm} (\dot{\mathbf{a}}_{mm}^H \mathbf{C}_{m,\mathrm{cmp}}^{-1} \dot{\mathbf{a}}_{mm}) \cdot (\mathbf{v}_{nm}^{'H} \mathbf{D}_n \mathbf{R}_\mathbf{X}^* \mathbf{D}_m^H \mathbf{v}_{mm}^{'})$$

$$+ L\alpha_{nm}\alpha_{mm} (\mathbf{a}_{mm}^H \mathbf{C}_{m,\mathrm{cmp}}^{-1} \dot{\mathbf{a}}_{mm}) \cdot (\mathbf{v}_{nm}^{'H} \mathbf{D}_n \mathbf{R}_\mathbf{X}^* \mathbf{D}_m^H \dot{\mathbf{v}}_{mm}^{'})$$

$$+ L\alpha_{nm}\alpha_{mm} (\dot{\mathbf{a}}_{mm}^H \mathbf{C}_{m,\mathrm{cmp}}^{-1} \dot{\mathbf{a}}_{mm}) \cdot (\mathbf{v}_{mm}^{'H} \mathbf{D}_m \mathbf{R}_\mathbf{X}^* \mathbf{D}_n^H \mathbf{v}_{nm}^{'})$$

$$+ L\alpha_{nm}\alpha_{mm} (\dot{\mathbf{a}}_{mm}^H \mathbf{C}_{m,\mathrm{cmp}}^{-1} \mathbf{a}_{mm}) \cdot (\dot{\mathbf{v}}_{mm}^{'H} \mathbf{D}_m \mathbf{R}_\mathbf{X}^* \mathbf{D}_n^H \mathbf{v}_{nm}^{'})$$

$$+ L\alpha_{nm}\alpha_{mm} (\dot{\mathbf{a}}_{mm}^H \mathbf{C}_{m,\mathrm{cmp}}^{-1} \dot{\mathbf{a}}_{mm}) \cdot (\mathbf{v}_{nm}^{'H} \mathbf{D}_n \mathbf{R}_\mathbf{X}^* \mathbf{D}_m^H \mathbf{v}_{nm}^{'}). \tag{12}$$

where $\mathbf{D}_m = \mathrm{diag}(\mathbf{0}_{N_t}, .., \mathbf{I}_{N_{tx}}, .., \mathbf{0}_{N_t}) \in \mathcal{C}^{N \times N}$; $\mathbf{v}_{mm}^{'} = [\vec{0}_{N_t}, .., \mathbf{v}_{mm}, .., \vec{0}_{N_t}] \in \mathcal{C}^{N \times 1}$ with $\vec{0}_{N_t}$ being an all-zero vector of N_t elements, and $\mathbf{C}_{m,\mathrm{cmp}} = \sigma_R^2 \mathbf{I}_{N_{rx}}$. The FIV for the two BSs, $F_{m,\mathrm{comp}}$, can be obtained by substituting (12) in (5). The corresponding optimization problem can be formulated as

$$(\mathrm{P2}): \underset{\{\mathbf{x}_s\}, \{\mathbf{R}_{\mathbf{X}_s}\}}{\mathrm{maximize}} \ \rho \, f + (1 - \rho)\gamma,$$

$$F_{m,\mathrm{comp}} \geq f, \quad \forall m, \tag{13a}$$

$$\begin{bmatrix} \mathbf{R}_{\mathbf{X}_s} & \mathbf{x}_s \\ \mathbf{x}_s^H & 1 \end{bmatrix} \geq 0; \ \mathbf{R}_{\mathbf{X}_s} \geq 0 \, \forall s, \tag{13b}$$

$$\sum_{k=1}^K \mathrm{tr}\left(\mathbf{D}_m \mathbf{w}_k \mathbf{w}_k^H \mathbf{D}_m^H\right) \leq P_t, \forall m. \tag{13c}$$

$$\left(\left|\mathrm{Im}\left\{\mathbf{h}_{ks}^T \mathbf{x}_s\right\}\right| - \left(\mathrm{Re}\left\{\mathbf{h}_{ks}^T \mathbf{x}_s\right\}\right)\tan\psi + \gamma^{'} \sigma_{\mathrm{C}} \frac{1}{\cos\psi}\right) \leq 0 \, \forall k, s \tag{13d}$$

The objective function of (P2) is the weighted combination of minimizing the maximum CRB and maximizing the minimum SINR values. Here, f represents the minimum FIV. Equation (13b) is the semi-definite relaxed (SDR) representation of the relation between $\mathbf{R}_{\mathbf{x}_{ms}}$ and $\mathbf{x}_{ms}$ using the Schur complement. Equation (13c) is the average power constraint per BS, and (13d) is the CI-based SINR condition derived from (3). Problem (P2) is a convex optimization problem and can be solved using Matlab's CVX.

The proposed optimization framework utilizes alternating optimization that alternates between maximizing the sensing and communication performances and minimizing the inter-cel interference (in the CBF scheme). The convergence of
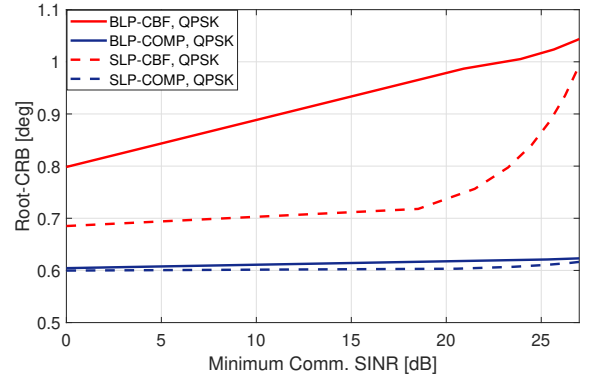

Fig. 3: RCRB Vs SINR with $N_t = 6$, $N_r = 6$, $K = 2$, $J = 2$, $f_c = 5.6$ GHz, $\theta_{11} = -50°$, $\theta_{12} = 60°$, $\theta_{22} = 50°$, $\theta_{21} = -60°$, $P_t/\sigma_{\mathrm{C}}^2 = P_t/\sigma_{\mathrm{R}}^2 = 10^4$, $\psi - 45°$, $I_{\max}^2/\sigma_{\mathrm{C}}^2 = 10$ and $M_{\mathrm{psk}} = 4$.

such an algorithm is proven in [15]. The main limitation of the proposed CoMP scheme is the associated overhead in sharing the data and CSI among the BSs and ensuring perfect synchronization between them. Furthermore, the proposed framework can be extended to any modulation schemes using the CI-based SINR formulations explained in [14].

IV. NUMERICAL EVALUATION

In this section, we summarize our main findings through numerical evaluation. The simulation parameters are $J = 2$, $K = 3$, $P_t = 40$ dBm; the noise variances $\sigma_{\mathrm{C}}^2 = \sigma_{\mathrm{R}}^2 = 0$ dBm. The targets are located at $\theta_{11} = -50°$, $\theta_{12} = 60°$, $\theta_{22} = 50°$, $\theta_{21} = -60°$. The communication channel gains are normalized such that the signal power received through an inter-cell link is considered to be reduced by a factor of 3. α_{mm} is selected such that the received SNR of the intra-cell echo signal: $|\alpha_{mm}|^2 L P_t/\sigma_{\mathrm{R}}^2 = 1$ [16], whereas $|\alpha_{nm}|^2 = |\alpha_{mm}|^2/3$.

Fig. 3 shows the root-CRB (RCRB)- γ trade-off for the considered four scenarios: BLP-CBF, BLP-CoMP, SLP-CBF, and SLP-CoMP. The BLP solutions serve as benchmarks against their SLP counterparts. As seen in the figure, the SLP technique outperforms the BLP counterparts: in the CBF scenario, the SLP technique utilizes the intra-cell interference constructively, thereby reducing the power needed to achieve the minimum SINR compared to the BLP technique, thus allowing the BS to radiate more power towards its target to improve the sensing performance. In the CoMP case, the SLP further improves the ISAC performance by utilizing intra-cell and inter-cell interference.

Fig. 4 shows the relative performance of the obtained SLP solutions under different modulation schemes, namely QPSK, 8-PSK, 16-PSK. As the order of the modulation increases, the CI region of a nominal constellation point diminishes. This reduction is reflected in the SINR constraint through ψ. A narrower CI requires the transmitter to allocate more power than a wider CI region. This degrades the sensing performance, as seen in the figure.
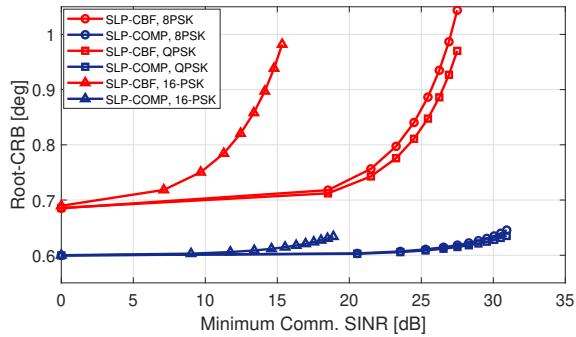
Fig. 4: RCRB Vs SINR $N_t = 6$, $N_r = 6$, $K = 2$, $J = 2$, $f_c = 5.6$ GHz, $\theta_{11} = -50°$, $\theta_{12} = 60°$, $\theta_{22} = 50°$, $\theta_{21} = -60°$, $P_t/\sigma_C^2 = P_t/\sigma_R^2 = 10^4$, $I_{max}^2/\sigma_C^2 = 10$.

V. CONCLUSION

We proposed a framework for designing an optimal transmit symbol vector that maximizes a weighted combination of the Fisher information value and minimum communication signal-to-interference-plus-noise-ratio (SINR) of a multi-cell integrated sensing and communication (ISAC) system. The BSs were allowed to coordinate at different levels by sharing channel state information (CSI) and inter-cell reflection directions or CSI, ICR direction, and user data. The respective scenarios are called coordinated beamforming (CBF) and coordinated multipoint(CBF). The numerical evaluations suggest that the additional received power through the ICR directions can enhance the ISAC performance in the CoMP scheme. In contrast, it should be suppressed in the CBF scheme. Moreover, the symbol-level precoding(SLP) that uses the interference in a constructive outperforms the block-level precoding counterparts.

REFERENCES

[1] F. Liu, C. Masouros, A. P. Petropulu, H. Griffiths, and L. Hanzo, "Joint Radar and Communication Design: Applications, State-of-the-Art, and the Road Ahead," *IEEE Trans. on Commun.*, vol. 68, no. 6, pp. 3834–3862, 2020.

[2] W. Chen, X. Lin, J. Lee, A. Toskala, S. Sun, C. F. Chiasserini, and L. Liu, "5g-advanced toward 6g: Past, present, and future," *IEEE Journal on Selected Areas in Communications*, vol. 41, no. 6, pp. 1592–1619, 2023.

[3] T. Wild, V. Braun, and H. Viswanathan, "Joint Design of Communication and Sensing for Beyond 5G and 6G Systems," *IEEE Access*, vol. 9, pp. 30 845–30 857, 2021.

[4] E. Björnson, E. Jorswieck *et al.*, "Optimal Resource Allocation in Coordinated Multi-cell Systems," *Foundations and Trends® in Communications and Information Theory*, vol. 9, no. 2–3, pp. 113–381, 2013.

[5] R. Li, Z. Xiao, and Y. Zeng, "Beamforming Towards Seamless Sensing Coverage for Cellular Integrated Sensing and Communication," in *2022 IEEE International Conference on Communications Workshops (ICC Workshops)*. IEEE, 2022, pp. 492–497.

[6] D. Xu, C. Liu, S. Song, and D. W. K. Ng, "Integrated Sensing and Communication in Coordinated Cellular Networks," *arXiv preprint arXiv:2305.01213*, 2023.

[7] Y. Xu, D. Xu, L. Xie, and S. Song, "Joint BS Selection, User Association, and Beamforming Design for Network Integrated Sensing and Communication," *arXiv preprint arXiv:2305.05265*, 2023.

[8] Y. Xu, L. Xie, D. Xu, and S. Song, "Fundamental Limits and Base Station Selection for Collaborative Sensing in Perceptive Mobile Networks," in *2023 IEEE International Mediterranean Conference on Communications and Networking (MeditCom)*. IEEE, 2023, pp. 97–102.

[9] W. Jiang, Z. Wei, F. Liu, Z. Feng, and P. Zhang, "Collaborative Precoding Design for Adjacent Integrated Sensing and Communication Base Stations," *arXiv preprint arXiv:2310.08246*, 2023.

[10] X. Liu, H. Zhang, K. Long, A. Nallanathan, and V. C. Leung, "Distributed Unsupervised Learning for Interference Management in Integrated Sensing and Communication Systems," *IEEE Transa. on Wireless Commun.*, 2023.

[11] N. Babu, C. Masouros, K.-K. Wong, and X. Kang, "Multi-cell Coordinated Joint Sensing and Communications," in *2023 Asilomar Conference*. IEEE, 2023.

[12] C. Masouros and G. Zheng, "Exploiting known interference as green signal power for downlink beamforming optimization," *IEEE Trans. on Signal Processing*, vol. 63, no. 14, pp. 3628–3640, 2015.

[13] K. L. Law and C. Masouros, "Symbol error rate minimization precoding for interference exploitation," *IEEE Transactions on Communications*, vol. 66, no. 11, pp. 5718–5731, 2018.

[14] A. Li, D. Spano, J. Krivochiza, S. Domouchtsidis, C. G. Tsinos, C. Masouros, S. Chatzinotas, Y. Li, B. Vucetic, and B. Ottersten, "A tutorial on interference exploitation via symbol-level precoding: Overview, state-of-the-art and future directions," *IEEE Communications Surveys & Tutorials*, vol. 22, no. 2, pp. 796–839, 2020.

[15] J. C. Bezdek and R. J. Hathaway, "Convergence of Alternating Optimization," *Neural, Parallel & Scientific Computations*, vol. 11, no. 4, pp. 351–368, 2003.

[16] F. Liu, Y.-F. Liu, A. Li, C. Masouros, and Y. C. Eldar, "Cramér-Rao Bound Optimization for Joint Radar-Communication Beamforming," *IEEE Transactions on Signal Processing*, vol. 70, pp. 240–253, 2022.